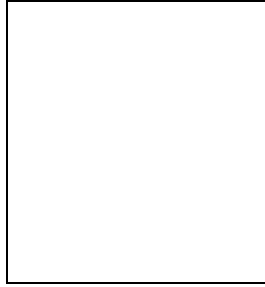


DØ STATUS AND FIRST RESULTS FROM RUN 2

AURELIO JUSTE

(on behalf of the DØ Collaboration)

Fermi National Accelerator Laboratory, P.O. Box 500, Batavia, IL 60510, USA



In order to fully exploit the physics potential of the Tevatron Run 2, the DØ detector has been upgraded. Having nearly completed the commissioning phase, the DØ detector is starting to produce its first physics results. An overview of the status of the main subdetectors involved in the upgrade is given, followed by some examples of preliminary physics results already emerging.

1 Introduction

Run 2 of the upgraded Tevatron collider started in March 2001. The ultimate goal is to accumulate $\sim 2 \text{ fb}^{-1}$ of integrated luminosity by 2005, which represents a twenty-fold increase with respect to Run 1. The center-of-mass energy has been increased from 1.8 TeV to 1.96 TeV and the bunch crossing interval reduced from $3.5 \mu\text{s}$ to 396 ns. In order to fully exploit the physics opportunities of the high luminosity Main Injector era, as well as to be able to cope with the higher event rates and backgrounds expected, the DØ detector has been upgraded¹. Run 2 offers an extremely exciting physics program which includes high statistics studies on the top quark sector, searches for the Higgs boson and new phenomena, precision electroweak measurements, b-physics and QCD.

2 Status of the DØ Detector

The upgrade builds on the strengths of the DØ detector, namely, excellent calorimetry and muon system and, most importantly, augments its tracking and triggering capabilities: new inner tracking system, new central and forward preshower detectors and a new pipelined 3-level trigger system. The inner tracking consists of a scintillating fiber tracker and a silicon

microstrip tracker, embedded in a 2 Tesla axial magnetic field, which is provided by a ~ 2.6 m long super-conducting solenoid with ~ 0.5 m inner radius.

The DØ detector was rolled into the collision hall in January 2001, with the first collisions being delivered in April 2001. During the summer 2001, the emphasis was put in commissioning and timing in the detector, as well as improving the electronics, data acquisition and offline reconstruction. In October 2001, during a six week shutdown, most of the central fiber tracker electronics were installed. As of March 2002, the accelerator has delivered $\sim 27 \text{ pb}^{-1}$ of integrated luminosity, of which $\sim 10 \text{ pb}^{-1}$ have been collected by DØ. A significant fraction ($\sim 25\%$) of this integrated luminosity has been devoted to detector commissioning.

An overview of the status of the main subdetectors involved in the upgrade is given below.

2.1 Silicon Microstrip Tracker (SMT)

The SMT is the innermost tracking element with a total of $\sim 800,000$ readout channels. It consists of six barrel modules with silicon sensors parallel to the beamline, as well as a total of 16 disks (four of them interspersed with the barrels) with silicon sensors normal to the beamline for forward tracking ($|\eta| \leq 3$). The barrels are 12.4 cm long and contain four concentric layers with radii ranging from 2.7 cm to 9.4 cm. The use of single- and double-sided (2° or 90° stereo view) sensors provides 3-D track reconstruction capabilities. The detector is fully commissioned, with the barrels and 12 innermost disks (4 outermost disks) being $\sim 95\%$ ($\sim 86\%$) operational.

2.2 Central Fiber Tracker (CFT)

The CFT spans the radial region $20 < r < 51$ cm and consists of eight concentric barrels of axial and stereo scintillating fiber doublets. The fibers, with $830 \mu\text{m}$ diameter, are read out through ~ 12 m long clear wave-guides down to Visible Light Photon Counters (VLPCs), a variant of the solid-state photomultiplier. VLPCs operate at 9K, and have high quantum efficiency ($\sim 85\%$) and excellent signal-to-noise ratio. The total number of readout channels is 77,000. The CFT also provides a fast track trigger at Level 1. The subdetector is close to being fully commissioned, with only missing readout boards for 48% of the stereo view. It is expected to be fully instrumented by mid-April 2002.

2.3 Calorimeter

The upgrade preserves the excellent Run 1 calorimeter, based on LAr sampling with U absorber, which is rather uniform in response, nearly compensating and has a good energy resolution and coverage up to $|\eta| \leq 4.2$. The front-end electronics is upgraded in order to accommodate for the reduced bunch spacing, while preserving the noise performance. The subdetector is fully commissioned and performing very well, with only $\sim 0.1\%$ of a total of 55,000 readout channels being dead or noisy.

2.4 Muon System

The upgrade is driven by the goal of maximizing the acceptance for muons from high- p_T processes, which implies extending the detector coverage up to $|\eta| \leq 2$ and having efficient, unprescaled triggers. Like for the calorimeter, the front-end electronics has also been upgraded. Tracking is performed by three layers of wire chambers, whose hits must be verified by corresponding coincidences in three layers of trigger scintillators with good granularity ($\Delta\eta \times \Delta\phi = 0.1 \times 4.5^\circ$ in the forward region) and time resolution ($\sigma \simeq 2.5$ ns). In order to reduce the fake trigger and track probabilities as well as aging effects, significant amount of shielding has been added. The subdetector is fully commissioned and giving an excellent performance.

3 First Physics Results

Over the course of 2001, significant progress was made in the development and verification of algorithms to identify physics objects: electrons, muons, jets, as well as to establish the electromagnetic and jet energy scales.

3.1 QCD Physics

The good performance of the calorimeter has allowed to perform preliminary studies on jet physics, such as the inclusive jet p_T spectrum (Fig. 1) or the dijet mass spectrum. Jets are reconstructed in the central region of the calorimeter ($|\eta| < 0.5$) with a cone algorithm with radius $R = 0.7$ in $\eta - \phi$ space. These spectra correspond to an integrated luminosity of ~ 1 pb $^{-1}$ and are not fully corrected: there is a preliminary correction for jet energy scale (but no unsmearing of resolution effects) and there is no correction for trigger or selection efficiencies.

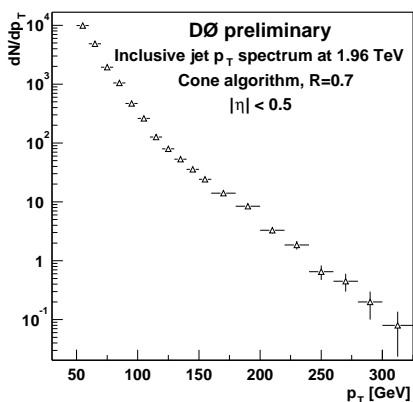


Figure 1: Inclusive jet p_T spectrum. See text for details.

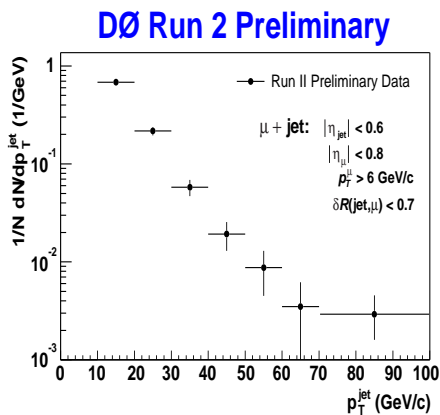


Figure 2: Inclusive jet p_T spectrum for events with a muon within the jet cone. See text for details.

3.2 B-Physics

The use of tracking allows to reconstruct particles into which B hadrons typically decay: $K_S^0 \rightarrow \pi^+\pi^-$, $\Lambda^0 \rightarrow p\pi^-$, $J/\Psi \rightarrow \mu^+\mu^-$, etc. Another preliminary result is the measurement of the inclusive jet p_T spectrum (Fig. 2) for events with a muon contained within a jet. This distribution corresponds to less than 0.2 pb $^{-1}$ and includes trigger and reconstruction efficiencies, as well as jet energy scale corrections. In order to obtain the inclusive b-jet p_T spectrum, the b-jet content in the sample can be estimated by using the large p_T of the muon relative to the jet axis to discriminate between direct $b \rightarrow \mu$ and backgrounds ($c \rightarrow \mu$ and $\pi/K \rightarrow \mu$).

3.3 Electroweak Physics

First preliminary results on electroweak physics include the development of dedicated selections for Z and W bosons. The selection of $Z \rightarrow e^+e^-$ events (Fig. 3) requires two isolated electromagnetic clusters in the calorimeter, with at least one of them matched to a global track (using both the SMT and the CFT) in order to reduce the dominant QCD backgrounds involving photons and π^0 s. This sample has been mainly used to determine the absolute energy scale ($m_{ee} = m_Z$) as well as to estimate the tracking efficiency. By requiring instead a single electromagnetic cluster matched to a global track and large missing E_T , a relatively clean sample

of $W \rightarrow e\nu$ candidates is selected, which shows in the transverse mass distribution of the $e + \nu$ the characteristic jacobian peak near m_W (Fig 4). Those candidate events with additional jets ($W(\rightarrow e\nu)+\text{jets}$) will constitute the main background for top-quark and Higgs boson analyses.

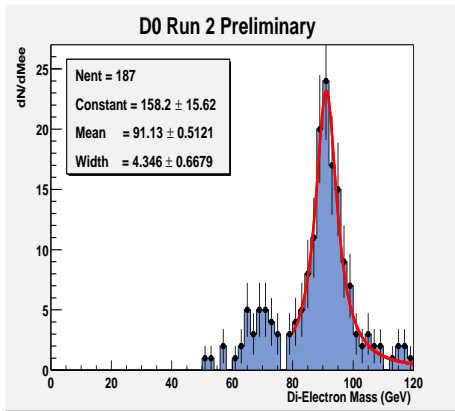


Figure 3: Di-electron invariant mass from $Z \rightarrow e^+e^-$ candidates after energy scale corrections.

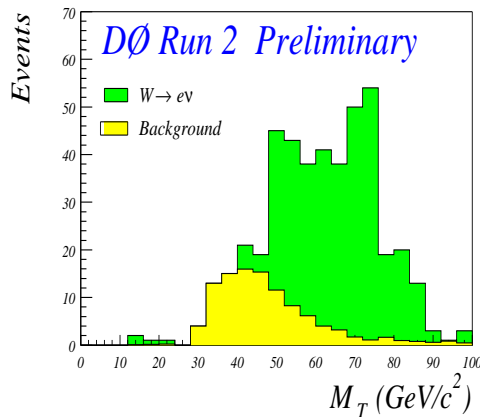


Figure 4: Transverse mass distribution for events containing a candidate $W \rightarrow e\nu$. The background, estimated from the data, consists mainly of QCD events with fake electrons.

3.4 New Phenomena Physics

The $D\bar{O}$ detector is particularly suited for searches for new phenomena physics involving jets, isolated leptons and missing E_T . Some preliminary results include the determination of the missing E_T resolution from the inclusive di-electron sample (an important signature in searches for e.g. extra dimensions, R-parity violating SUSY, etc), and searches for trileptons and first generation leptoquarks, which have yielded some candidate events.

4 Conclusions

The Tevatron Run 2 started in March 2001, offering one of the most exciting physics program of this decade. Over the course of 2001, enormous progress has been made at $D\bar{O}$ in terms of detector commissioning. Preliminary performance results are encouraging and indicate that the upgraded $D\bar{O}$ detector will be able to fully exploit the available physics opportunities. Despite the small amount of integrated luminosity delivered so far, first physics results are already emerging. The expected optimization of the detector, trigger and data acquisition performances as well as improvements in calibration, alignment, event selection and reconstruction techniques give an impressive outlook.

Acknowledgments

The author would like to thank Professor J. Tran Thanh Van and the conference organizers for an stimulating and enjoyable conference.

References

1. $D\bar{O}$ Collaboration, FERMILAB-PUB-96-357 (1996).